Experimental and numerical study on the wavy instability in a Rayleigh-Bénard-Poiseuille flow: non linear effects.

F. Seychelles, S. Mergui, Xavier Nicolas

Experimental and numerical study on the wavy instability in a Rayleigh-Bénard-Poiseuille flow: non linear effects.

F Seychelles[1], **S Mergui**[1,3], **and X Nicolas**[2]

[1]UPMC Université Paris 06, FAST UMR CNRS 7608, Bat 502, Campus Univ, Orsay, F-91405, France
[2]Université Paris-Est, MSME UMR CNRS 8208, 5 bd Descartes, Marne-La-Vallée, F-77454, France

E-mail: mergui@fast.u-psud.fr

Abstract. A combined experimental and numerical study of a Rayleigh-Bénard-Poiseuille air flow in a rectangular channel is presented. The aim of the present paper is to characterize a secondary instability, referred to as wavy instability and known to be a convective instability, with the objective to identify the best situation for an optimal homogenization of heat transfers in the system. A periodic mechanical excitation is introduced at channel inlet and the spatial and temporal evolution of the temperature fluctuations are analyzed, depending on the Rayleigh number, the frequency and the amplitude of the perturbation. The Reynolds number is fixed. As the saturated state is a priori the best situation to homogenize the transfers, the objective is to expand the saturation area and to generate a maximum saturation amplitude value. It is shown that the best choice is a high Rayleigh number or/and a large magnitude of perturbation associated with a specific low value of the forcing frequency.

1. Introduction

The present paper is concerned with an experimental and 3D numerical study on a Rayleigh-Bénard-Poiseuille (RBP) air flow in a horizontal rectangular channel heated from below and cooled from above. RBP flows are present in industrial applications, for example during the Chemical Vapor Deposition process used to obtain thin solid films or coatings on substrates [1] or in the framework of electronic component cooling. It is of great interest to characterize the flow structures in such systems, the objective being to control the magnitude and the homogeneity of the heat and mass transfers.

In RBP configuration, the basic flow consists in a purely conducting Poiseuille flow. Many convection patterns resulting from successive destabilization of the basic flow are observed, depending on the characteristic parameter values (Reynolds, Rayleigh and Prandtl numbers and channel transversal aspect ratio). For example, steady parallel convection rolls oriented in the direction of the mean flow, referred to as longitudinal rolls, are observed for Rayleigh numbers above a critical value and for sufficiently high Reynolds numbers (typically $Re > o(10)$ in air). Here we focus on a secondary unsteady instability arising from the destabilization of the longitudinal rolls [2]. In previous studies ([3], [4]), we showed that a wavy pattern can develop in the channel provided that a perturbation is imposed to the flow meaning that the wavy mode is convectively unstable.

[3] whom any correspondence should be addressed.

In the present study, the purpose is to characterize both experimentally and numerically the spatial and temporal behaviour of this secondary instability in order to identify the most effective conditions to homogenize the heat transfer at the walls. Time and spatial evolution of the temperature fluctuations along the channel are analyzed to characterize the sensitivity of the flow to a periodic forcing. The three control parameters used in this study are: the Rayleigh number, the frequency and the amplitude of the excitation. The transverse aspect ratio of the channel is B = W (width) / H (height) = 10 and the Reynolds and Prandtl numbers are fixed at Re = 175 and Pr=0,71.
The experimental set up and the numerical code are described in §2 and §3, respectively, and the results are presented in §4. First the influence of the amplitude of the excitation on the wavy instability is discussed following by the influence of the Rayleigh number. Finally the influence of the forcing frequency is addressed.

2. Experimental set up

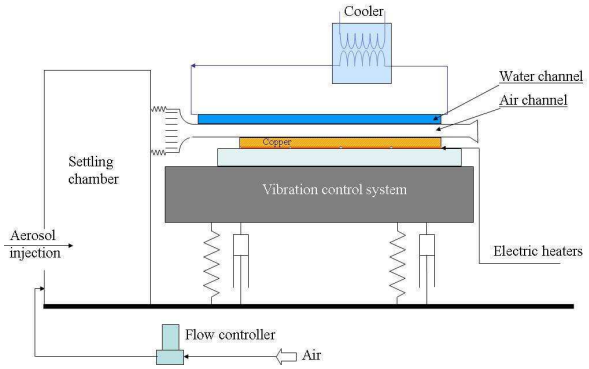

Figure 1. Sketch of the experimental set up.

The experimental channel is divided into three parts: (i) an unheated zone of 50 cm length located upstream the heated zone allowing for the development of the Poiseuille flow, (ii) the heated region, (iii) an unheated zone of 40 cm placed downstream to minimize exit effects. The length of the heated region is L=2 m, designed so as to allow for a fully developed vortex flow for a large range of parameters, $30 \leq Re \leq 300$ and $Ra \leq 12000$. The lateral walls of the channel are made of polycarbonate plates. The lower plate of the test section is made of a 10 mm thick copper plate maintained at a constant temperature using five independent electric heaters. The upper plate of the test section is made of 5 mm thick polycarbonate sheet maintained at a constant temperature using water circulation in a channel above it. The dimensions of the channel are $W \times H = 15\ cm \times 1.5\ cm$ providing a transverse aspect ratio B = W/H = 10.
For the range of temperature considered in this paper, the relative error on the Rayleigh number value is estimated to be less than 10 percent. The relative error on the Reynolds number value is estimated to be less than 6 percent. The detailed analysis is available in [3].
The wavy instability is investigated by studying the response of the flow to a permanent quasi-harmonic excitation introduced at the beginning of the heated zone. The apparatus has been designed to impose a perturbation with a controlled frequency and amplitude. The system consists in a 1 mm diameter horizontal rod that oscillates in the spanwise direction, parallel to itself. It is located perpendicular to the flow at channel mid-height over the whole width of the channel and is driven by a crank disk. The oscillating movement of the rod, $d_{rod}(t)$, is characterized by its amplitude and the forcing frequency, f^*, and is given by the relation:

$$\frac{d_{rod}(t)}{H} = d\,\sin\left(2\pi\ f^*\ t\right) + d_1\,\sin\left(2\pi\ (2f^*)\ t\right) + d_2\,\sin\left(2\pi\ (3f^*)\ t\right)$$

Several crank disks are used to impose various values of d, from 0.14 to 1.4 (i.e. $d^* = d\,H$ from 2.1 mm to 20.7 mm). The characteristics of the displacements associated with the crank disks mainly used in the present study are reported in Table 1.

Table 1. Amplitude of displacement generated by the crank disks.

	Disk 1	Disk 2	Disk 3	Disk 4
fundamental d	1.01	0.75	0.41	0.14
harmonic 1 d1	0.10	0.05	0.01	
harmonic 2 d2	0.006	0.003		

Measurements of the frequency and of the amplitude of the oscillations all along the channel are performed using a Chromel-Alumel thermocouple of 135 μm in diameter located at channel mid-height at a given distance from the lateral walls (see figure 2) and moving in the longitudinal direction, from $x^* = 20$ cm to $x^* = 190$ cm (i.e. $x = x^*/H = 13$ to $x = 127$).
For each point of measurement, we acquire 10 samples of at least 80 periods of the fundamental mode. A discrete Fourier Transform is then performed using a signal of duration corresponding to a multiple of the period of the mode under consideration (fundamental and harmonics). With this condition, the amplitude of the mode is directly related to the height of the peak of the Fourier spectra [5].
Figure 3 displays an example of a signal delivered by the thermocouple and the mean of the Fourier spectra. We can detect four amplified modes: a predominant peak corresponding to the forcing frequency and the three first harmonics.

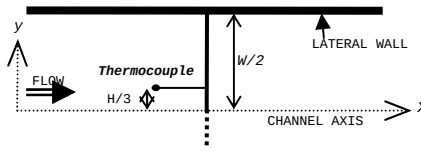

Figure 2. Location of the thermocouple in the horizontal plane at channel mid-height.

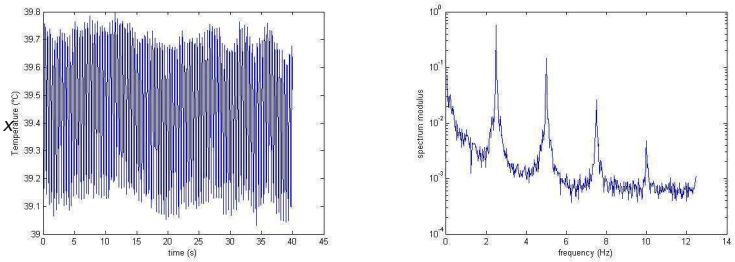

(a) (b)

Figure 3. (a) Time evolution of the signal delivered by the thermocouple located at x = 120, (b) modulus of the discrete Fourier transform (average over 10 samples). Forcing frequency $f^* = 2.5$ Hz, forcing amplitude d = 0.41, Ra = 10000, Re = 175.

Because of its inertia, the thermocouple does not respond instantly or with a perfect fidelity to a change in its environment. By considering a simplified heat balance for the thermocouple subjected to a periodic change in the environment temperature (from $+T_e$ to $-T_e$) and assuming that all the heat transferred to the thermocouple is by convection, a first order estimate of the ratio of the thermocouple amplitude to that of the environment (attenuation factor) is given by [6]:

$$R(f_e) = \frac{T_{\max}}{T_e} = \frac{1}{\left(1 + (2\pi\ f_e\ \tau)^2\right)^{0.5}}$$

where f_e is the frequency of the environmental oscillations and $\tau = \rho_{th} c_{th} D/(6h)$ is the time constant of the thermocouple, where D, ρ_{th} and c_{th} are the diameter, density and specific heat capacity of the thermocouple, respectively, and h is the convective heat transfer coefficient of the flow surrounding the thermocouple. Radiation and conduction effects on the thermocouple response have been found to be negligible. The convective coefficient is calculated from the Nusselt number correlation reported in [7] related to heat transfer from a sphere:

$$Nu = 2 + \left(0.4\ \mathrm{Re}_D^{1/2} + 0.06\ \mathrm{Re}_D^{2/3}\right)\mathrm{Pr}^{0.4}$$

In our case, $\mathrm{Re}_D = 1.58$ and $\mathrm{Pr} = 0.71$, leading to a time constant $\tau = 190$ ms. The attenuation factor $R(f_e)$ is in the range $0.22 < R(f_e) < 0.63$ for $1\ \mathrm{Hz} < f_e < 3.5\ \mathrm{Hz}$. All the experimental temperature fluctuation values, A, presented in this paper have been modified as follows: $A = A_{measure} / R(f_e)$, where $A_{measure}$ is the measured response of the thermocouple.

3. Physical problem and mathematical model

The channel considered to simulate the PRB flows is shown in Fig. 4. It is a horizontal rectangular channel of height H, width W and length L, heated from below. A fully developed Poiseuille flow enters into the channel at the cold temperature T_c, with an average velocity U_{mean}. After an adiabatic entrance zone of length L_e, the top wall is maintained at T_c and the bottom wall is heated at a higher temperature T_h. The vertical lateral walls are adiabatic all along the channel. The origin of the reference frame being placed at the beginning of the heated plate, the computational domain is defined by $(x,y,z) \in [-A_e, A-A_e]\times[0, B]\times[0, 1]$ in dimensionless Cartesian coordinates, where A=L/H and B=W/H are the streamwise and spanwise aspect ratios of the channel and $A_e=L_e/H$ is the streamwise entrance aspect ratio. In this study, B = 10, A_e = 1 and A = 200.

We consider PRB flows of incompressible Newtonian fluids, governed by the 3D Navier-Stokes equations under the Boussinesq approximation. This assumption is justified here since, in the present experiments, the maximum temperature difference in the air flow is 40°C at Ra=10000. Giving the reference quantities H, U_{mean}, ρU_{mean}^2, and H/U_{mean}, for the lengths, velocity, pressure and time respectively, and defining the reduced temperature $\theta=(T-T_c)/(T_h-T_c)$, the dimensionless governing equations for continuity, momentum and energy read as follows:

$$\nabla.\vec{v} = 0 \tag{1}$$

$$\frac{\partial \vec{v}}{\partial t} + (\vec{v}.\nabla)\vec{v} = -\nabla p + \frac{1}{Re}\nabla^2\vec{v} + \frac{Ra}{Re^2\,Pr}\theta\,\vec{k} \tag{2}$$

$$\frac{\partial \theta}{\partial t} + \vec{v}.\nabla\theta = \frac{1}{Re\,Pr}\nabla^2\theta \tag{3}$$

where $\vec{v} = (u,v,w)$ is the dimensionless velocity vector, $\vec{k}$ the upward unit vector and p the deviation of the mixture pressure from the hydrostatic pressure. $Ra=g\beta(T_h-T_c)H^3/(\nu\alpha)$, $Re= U_{mean}H/\nu$ and $Pr=\nu/\alpha$. The boundary conditions are:

at $x=-A_e$, $u=u_{Pois}(y,z)$, v=0 or sinusoidal excitation at channel mid-height, w=0, θ =0 (4)

at y=0 and B, $\vec{v} = \vec{0}$, $\partial\theta/\partial y = 0$ (5)

at z=0 and 1, for $x\in[-A_e,0]$, $\vec{v} = \vec{0}$, $\partial\theta/\partial z = 0$ (6)

at z=1, for $x\in[0, A-A_e]$, $\vec{v} = \vec{0}$, θ=0 (7)

at z=0, for $x\in[0, A-A_e]$, $\vec{v} = \vec{0}$, θ=1 (8)

at $x=A-A_e$, $\partial f/\partial t + \partial f/\partial x = 0$ for f=u, v, w and θ (9)

At the inlet, the analytical expression of the Poiseuille profile, $u_{Pois}(y,z)$, is given in [4]. At the outlet, the Orlanski type boundary conditions are used.

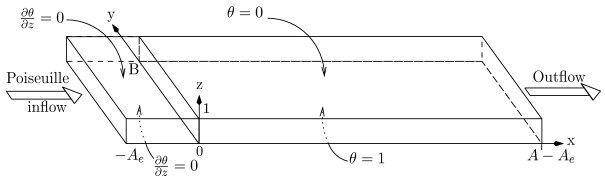

Figure 4: Dimensionless geometry and boundary conditions.

The problem (1-9) is solved using a finite difference method optimized for vectorial computers [4]. The equations are discretized in space on uniform, Cartesian and staggered grids using a centred scheme. The second-order Adams-Bashforth scheme is used for the time discretization. The dimensionless cell sizes and time step are $\Delta x\times\Delta y\times\Delta z=0.1\times0.05\times0.029$ and $\Delta t=0.01$. The time integration and the velocity-pressure coupling are solved by a projection method based on Goda's algorithm. The Helmholtz equations are solved using an incremental factorization method of ADI type which permits to keep a second order time accuracy. The Poisson equation for the pressure increment is solved by a factorization method. The linear systems resulting from these two factorization methods are all tridiagonal and are solved by the TDMA algorithm. A detailed description of this code, its validations and its performances can be found in [4].

Each simulation is divided into three steps: first, a longitudinal roll flow is simulated without any excitation, starting from a cold Poiseuille flow as initial condition and imposing $\theta=1$ at $z=0$, $x\in[0, A-A_e]$ for $t>0$. In the second step, a permanent sinusoidal excitation is introduced on the transversal velocity component, v, at mid-height of the inlet Poiseuille profile to approximately simulate the transversal oscillations of the horizontal rod placed in the experimental channel: at $x=-A_e$, $\forall y\in[0, B]$ and $\forall z\in[0, 1]$ $v=0$, except at $z=0.5$ where $v=d\times 2\pi f\times\cos(2\pi ft)$ with f the dimensionless frequency and d the dimensionless excitation magnitude. The second step ends when fully developed wavy rolls are present in the whole channel. In the third step, the sinusoidal excitation is maintained at the inlet and the fully developed wavy roll flow goes on propagating through the channel. The third step provides the time signals that are recorded to characterize the fully-developed wavy roll flows that develop from the inlet excitation: the temperature θ is recorded at each time step, during 30,000 iterations, all along the streamwise line at (y, z)=(B/2-1/3, 0.5). These time signals are analyzed through Fourier transforms to determine the space variation of the Fourier spectra in the wavy roll flows. Since $\Delta t=0.01$ and the dimensionless recording duration is $t_{max}= 300$, the highest frequency, f_{max}, and the frequency step, Δf, of the Fourier spectra are: $f_{max}=1/(2\Delta t)=50$ and $\Delta f=1/t_{max}=3.33\times10^{-3}$. As we are going to see, the fundamental frequencies in the Fourier spectra vary between 0.18 and 0.27, which means that the recorded signals comprise at minimum 54 periods and that one period comprises at minimum 370 time steps. We have checked that this is enough to provide a Fourier analysis independent on Δt and the time signal duration.

4. Results

In this paper, the Reynolds number and the Prandtl number are fixed at Re = 175 and Pr = 0.71, respectively. The parameters used for comparisons between experimental and numerical results are specified in Table 2.

Table 2. Parameters used in the comparisons between the experimental and numerical results

Ra	ε	d	f
8000	1.5	0.14	0.23
		0.41	
		0.75	
10000	2	0.14	0.18
			0.23
			0.27
		0.41	0.23
		0.75	0.23

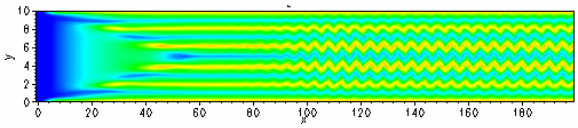

(a) ε = 1.5 ; f = 0.23 ; d = 0.14

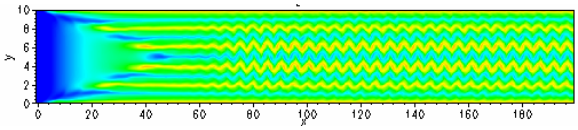

(b) : ε = 2 ; f = 0.23 ; d = 0.75

Figure 5. Instantaneous temperature field at channel mid-height resulting from periodic excitations at the inlet of the heated zone. The flow is coming from left to right. 10 rolls gradually develop from the inlet.

The parameter ε is defined as $\varepsilon=\left(\mathrm{Ra}-\mathrm{Ra}^*\right)/\mathrm{Ra}^*$, where Ra^* corresponds to the critical Rayleigh number obtained from the linear stability analysis of longitudinal rolls in a channel with transverse aspect ratio B = 10 [8]: Ra^* =3300 at Re = 175.

Figure 5 displays typical temperature fields obtained by the numerical code in the horizontal plane at channel mid height for two cases. We clearly observe the well-known development zone where ten longitudinal rolls gradually develop from the lateral walls [9], followed by the onset and growth of a wavy pattern. The main difference between the two figures concerns the feature of the development zone in the first part of the channel which is much shorter in case (b). The aim of the study reported in the next sections is to quantify the effect of the control parameters on the magnitude of the oscillations and on the development zone of the wavy pattern, specifically the length from the inlet at which the saturation amplitude is reached.

4.1. Influence of the excitation amplitude

Figure 6 displays the evolution of the temperature fluctuations along the channel obtained both experimentally and numerically for the two Rayleigh numbers under consideration and with d = 0.14, 0.41 and 0.75. The forcing frequency is fixed at f = 0.23. These curves can be divided into three distinct zones clearly visible for ε = 1.5. The first one corresponds to the development zone of the longitudinal rolls, where the evolution is not monotonic (for example in (a) for $0 < x < 60$). The second one corresponds to an exponential growth of the oscillation magnitudes (for example in (a) $60 < x < 85$) and the last one corresponds to a saturation zone where the amplitudes of the oscillations (fundamental and harmonics) no longer evolve and have the same level for all values of the excitation amplitude. For ε = 2 the exponential growing zone is very small and spatial oscillations of the mode amplitudes are detected for both the fundamental and the harmonics for all values of x.

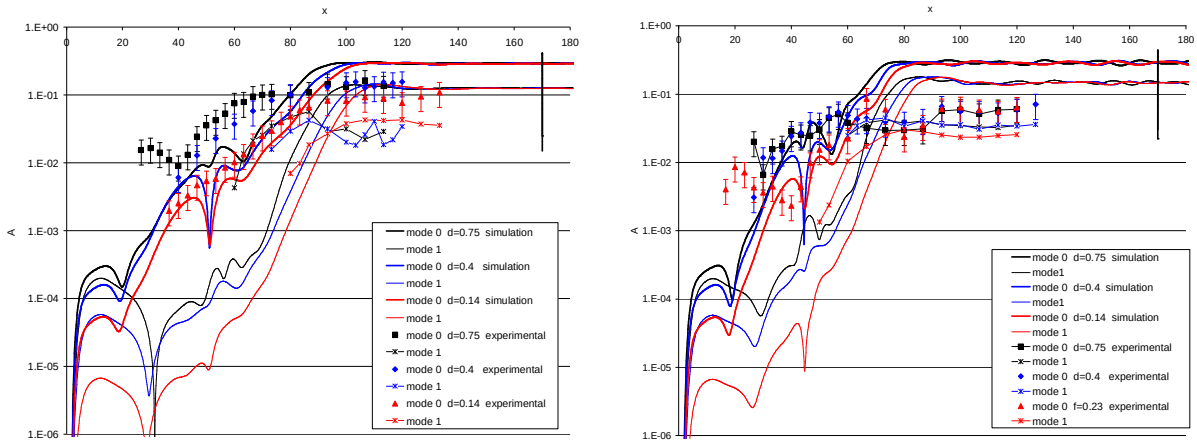

(a) ε = 1.5 (b) ε = 2

Figure 6. Influence of the excitation amplitude on the evolution of the temperature fluctuations along the channel: experimental and numerical results. f = 0.23. d = 0.14. The vertical bar at x = 170 indicates the variation range of the temperature fluctuation magnitude (fundamental mode) observed numerically when the transverse location, y, of the monitor point moves through the 5th roll (central part of the channel).

Experimental measurements are mainly performed downstream the development zone of the longitudinal rolls. However, the few points obtained in this zone are clearly above the numerical one. This is probably due to the presence of an intrinsic non-zero level of noise in the apparatus. For ε = 1.5, saturation is reached only for the fundamental mode for d = 0.41 and 0.75 and at the end of the experimental channel. The exponential growing zones develop earlier in the experiments than in the simulations but compare well if we consider the slopes of the curves meaning that the spatial growth rates in the linear regime are consistent. The saturation lengths are also similar for the fundamental mode at ε = 1.5: in both cases $x \approx 110$. The discrepancy in the saturation magnitudes observed between the experimental and numerical results is mainly due to the lack of control of the thermocouple position relative to the convection rolls. Indeed, numerical simulations show a large change in the temperature fluctuation magnitudes depending on the transverse position, y, of the monitor point relative to a roll for a given (x, z) location, as illustrated by the vertical bars at x=170 in figure 6. In experiments, we carefully control the thermocouple position relative to the channel walls but the convection rolls arrangement inside the domain results from complex interactions during the development stage and is not controlled by the operator.

Finally, the only effect of increasing the excitation amplitude *d* on the evolution of the wavy pattern is to slightly decrease the saturation length.

4.2. Influence of the Rayleigh number

The effect of the Rayleigh number on the evolution of the temperature fluctuations along the channel is reported in figure 7. An increase of the Rayleigh number leads to a decrease of the saturation length. More surprising is the fact that the magnitude of the saturation amplitudes related to the fundamental mode is independent of the Rayleigh number even if there is a difference in behaviour in the development zone. On the other hand, the discrepancy observed for the saturation amplitudes of the harmonics shows that the non linear effects become stronger when increasing the Rayleigh number.

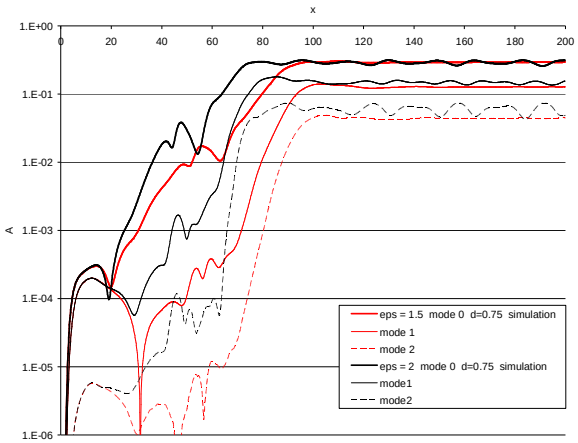

Figure 7. Influence of the Rayleigh number on the evolution of the temperature fluctuations along the channel. f = 0.23.

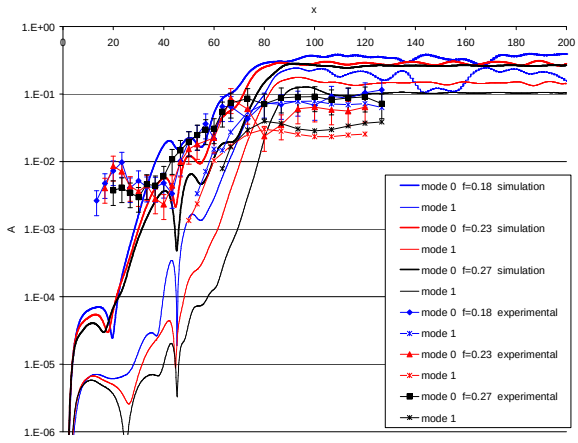

Figure 8. Influence of the forcing frequency on the evolution of the temperature fluctuations along the channel: experimental and numerical results. ε = 2, d = 0.14.

4.3. Influence of the frequency of the inlet perturbation

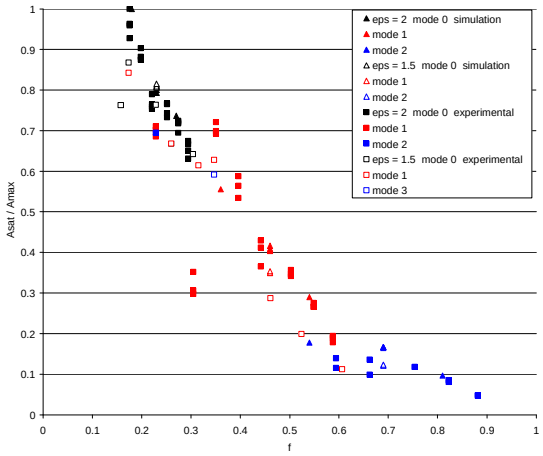

Figure 9. Influence of the forcing frequency on the normalized saturation amplitude. Comparison between experimental and numerical results.

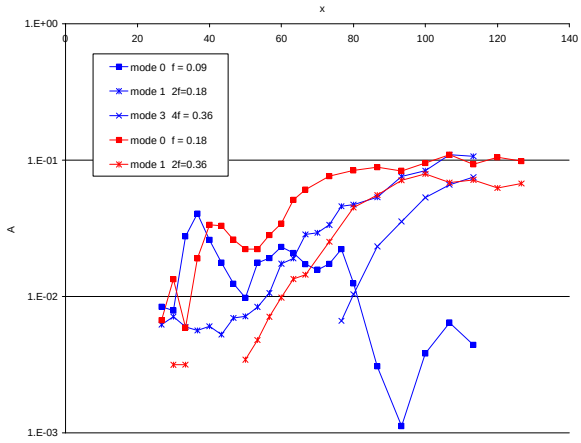

Figure 10. Evolution of the temperature fluctuations along the channel. Experiments. ε = 1.5, d = 1, f = 0.09 and 0.18.

The effect of the forcing frequency on the evolution of the temperature fluctuations along the channel is reported in figure 8 for ε = 2 and d = 0.14. We note that the saturation amplitudes are clearly dependent of the frequency of the oscillations. In experiments the oscillation amplitudes related to the fundamental modes are independent of the forcing frequency in the development zone while they are smaller when the forcing frequency is greater in simulation. A normalized saturation amplitude is

defined as the ratio between the saturation amplitude, A_{sat}, measured at the end of the channel at a given frequency, to the maximum saturation amplitude that is reached for f = 0.18, both in experiments and simulation. Figure 9 displays this normalized saturation amplitude as a function of the excitation frequency. The values reported in this figure for the experiments at ε = 1.5 correspond to an excitation amplitude d = 1. For f < 0.18, the saturation state is not reached for the fundamental mode, due to the growth of the more unstable first harmonic. This can be seen in figure 10 which displays the evolution of the temperature fluctuations in experiments for f = 0.09 and 0.18. It can be noted in Figure 9 that the experimental and numerical results compare very well. Thus, even if the saturation amplitudes are different between the two approaches, the wavy pattern behaves in the same way with respect to the control parameters.

5. Conclusion

In this paper, we studied a secondary wavy instability by analyzing the temporal and spatial evolution of the temperature fluctuations along the channel with the aim to identify the set of control parameters leading to an optimal homogenization of heat transfers in the system. This study was based on the fact that the wavy instability is a convective instability which was investigated by studying the response of the flow to a continuous periodic excitation introduced at the beginning of the heated zone. The control parameters used in this study were the Rayleigh number, the frequency and the amplitude of the perturbation. The Reynolds number was fixed at Re = 175.

It has been shown that the spatial evolution of the flow can be divided into three stages: (i) the development of longitudinal rolls, (ii) the onset and growth of the temperature fluctuations linked with the wavy pattern, (iii) the saturation of the oscillations. As the saturated state is a priori the best situation to homogenize the transfers, the objective was then to expand the saturation zone and to generate a maximum saturation amplitude value. We showed that the extent of the saturation zone increases when the amplitude of the perturbation or/and the Rayleigh number increases. On the other hand, the saturation amplitude is independent of the Rayleigh number and is maximal for a characteristic dimensionless frequency equal to 0.18, also independent of the Rayleigh number (at least in the range under study). Thus the best choice is a high Rayleigh number and a sufficiently large perturbation magnitude to enlarge the saturation zone and a specific low forcing frequency to allow a maximum value of the saturation amplitude. The investigation of the effect of the Reynolds number is now required to complete the study. A preliminary study showed that the Reynolds number acts on the saturation amplitude value and it would be of interest to study its influence on the most efficient forcing frequency.

ACKNOWLEDGMENTS

This work was granted access to the HPC resources of IDRIS under the allocations 2012-1474 made by GENCI (Grand Equipement National de Calcul Intensif).

REFERENCES

[1] Nicolas X, Benzaoui A and Xin S 2008 *J. Crystal Growth* **310** 174-186
[2] Clever R M and Busse F H 1991 *J. Fluid Mech*. **229** 517-529
[3] Pabiou H, Mergui S and Bénard C 2005 *J. Fluid Mech*. **542** 175-194
[4] Benzaoui A, Nicolas X and Xin S 2005 *Numer. Heat Transf. B* **48** 277-30
[5] Bergé P, Pommeau Y and Vidal C 1988 L'Ordre Dans le Chaos 5th Edition Paris Hermann
[6] Benedict R P 1984 Fundamentals of Temperature, Pressure and Flow Measurements, 3rd Ed. Wiley
[7] Whitaker S 1972 *AIChE Journal* **18** 361-371
[8] Nicolas X, Xin S and Zoueidi N 2010 *14th Int. Heat Transfer Conference*, Washington, DC, USA, 8-13 août 2010, Paper no. IHTC14-22256, **7** 203-208
[9] Mergui S, Nicolas X and Hirata S 2011 *Phys.of Fluids* **23** 084101